

Effect of electrolytic MnO₂ pretreatment on performance of as-prepared LiMn₂O₄

ZHAO Yu-qian¹, JIANG Qing-lai², WANG Wei-gang³, DU Ke³, HU Guo-rong³

1. School of Geosciences and Info-Physics, Central South University, Changsha 410083, China;
2. Powder Metallurgy Research Institute, Central South University, Changsha 410083, China;
3. School of Metallurgical Science and Engineering, Central South University, Changsha 410083, China

Received 12 December 2011; accepted 23 February 2012

Abstract: To investigate the effect of electrolytic MnO₂ (EMD) on the performance of LiMn₂O₄, several pretreatment methods, such as acid treating, presintering and impregnating with chromic salt, were used. The pretreated EMD and prepared LiMn₂O₄ were characterized by X-ray diffraction and inductively coupled plasma emission spectrometry. Charge and discharge tests of Li/LiMn₂O₄ batteries were also employed to evaluate electrochemical performance. The experimental results show that inorganic impurity contents in EMD decrease remarkably after acid treating; presintering EMD can remove adsorbent water and organic impurity, enlarge pore space and increase active reaction sites; pre-doping chromium in EMD can form more homogenous compound substance LiCr_{0.05}Mn_{1.95}O₄, which shows better structural stability and capacity retention.

Key words: lithium-ion batteries; cathode material; LiMn₂O₄; MnO₂

1 Introduction

Lithium-ion batteries, owing to their high energy and power density, have been used in a wide variety of portable electric devices, hybrid electric vehicles and many power supplies. The capacity of lithium-ion batteries is usually limited by cathode, and the cathode materials used in Li-ion batteries are mainly LiCoO₂, LiNiO₂, and LiMnO₂, with layered structure, and their ramifications, spinel LiMn₂O₄, olivine LiFePO₄, etc [1–3]. Among them, spinel LiMn₂O₄ is considered the preferred cathode material for lithium ion batteries because of its merits, such as low cost, high voltage platform, high-rate charge–discharge capacity, easy processing, and environmental friendliness [4–8]. However, its application is limited by its instability caused by Jahn-Teller effect and dissolution of manganese into electrolyte during the charge–discharge cycle [9,10]. To date, a variety of doping and coating techniques have been explored to control the structure and hence improve the electrochemical properties of LiMn₂O₄ [11].

Preparation methods and raw materials have great

influence on the structure and performance of cathode materials. There are two methods for spinel LiMn₂O₄ preparation: solid-state method and wet-chemical method. Solid-state method has been adopted widely because of its simple process, easily controllable condition, and being suit for industrialization. In a typical solid-state method to produce LiMn₂O₄, EMD and Li₂CO₃ are chosen as the raw materials. Here, MnO₂ can be looked as the frame of LiMn₂O₄ and its properties, such as structure, chemical composition, grain size, morphology, have great influence on the structure and performance of as-prepared spinel LiMn₂O₄ [12]. EMD is mostly produced to satisfy the demands for its role in disposable alkaline manganese battery. There are now few literatures for the researches on EMD pretreatment for the synthesis of LiMn₂O₄. In this work, the effect of EMD pretreatment on the performance of as-prepared LiMn₂O₄ is studied.

2 Experimental

2.1 Preparation of materials

In acid treating, EMD was immersed in 1 mol/L H₂SO₄ solution for 24 h and washed with purified water

copiously, then dried under 120 °C. The obtained EMD was named as A-EMD.

In presintering, EMD was heated under 400 °C for 6 h. The obtained EMD was named as H-EMD.

In impregnating with chromic salt, EMD was immersed in 50% (CH₃COO)₃Cr solution for 10 d to make Cr³⁺ ions infuse into the EMD pores, dried, and then heated under 400 °C for 6 h. The obtained EMD was named as C-EMD.

Spinel LiMn₂O₄ was prepared by a solid-state reaction from a stoichiometric mixture of Li₂CO₃ (99.9% in mass fraction) and electrolytic MnO₂ (Mn content of 59.6%) at 770 °C for 12 h. The as-prepared samples were named as A-EMD-LMO, H-EMD-LMO, and C-EMD-LMO from A-EMD, H-EMD, and C-EMD, correspondingly.

2.2 Characterization of materials

The phase identification of samples was carried out by powder X-ray diffraction (XRD, D/max 2550VB, Cu K_α, 40 kV, 250 mA, 10°–80°, Japan). Elementary content was analyzed by inductively coupled plasma emission spectrometry (ICP, Baird Corp. America).

The cathode materials were assembled into 2025-coin type cells to evaluate the electrochemical performance. The cathodes were prepared with slurry consisting of 80% (mass fraction) active materials, 10% conductive acetylene black and 10% polyvinylidene fluoride (PVDF) binder in N-methyl-2-pyrrolidone (NMP) solvent. This mixture was then tape-cast by a doctor blade on an aluminum foil current collector and dried at 120 °C for 12 h in a vacuum oven. The coated cathode foil was then cut into circular discs of 10 mm in diameter. The coin cells were assembled using 2025-stainless steel coin-type containers in an argon-filled glove box. Lithium foils were served as the anode and reference electrode, 1 mol/L LiPF₆ dissolved in 1:1 in volume ratio ratio of ethylene carbonate and dimethyl carbonate (EC: DMC) was used as the electrolyte, and a thin polypropylene film (Celgard 2400) acted as the separator. The charge–discharge cycles were

performed using LAND battery test system with a current density of 29.6 mA/g (0.2C) in the voltage range of 4.3–3.2 V at room temperature.

3 Results and discussion

3.1 Effect of pretreatment method on structure and chemical composition of EMD

Figure 1 shows the X-ray diffraction patterns of EMD, A-EMD and H-EMD. For the diffraction pattern of EMD without any treatment, some wide and symmetrical diffraction peaks of 2θ at about 22.1°, 37.2°, 42.6°, 56.3°, 67.4°, etc. can be observed. Compared with the diffraction peaks of ideal ramdellite-MnO₂, EMD shows a wider (130) peak with hiding in (021) peak at 2θ≈37°, which shows typical character of micro-twins defect. This structure of EMD belongs to γ-MnO₂ type, which features in the disordered alternate growth of the unit cells of pyrolusite and ramdellite [13] (shown in Fig. 2).

The structure of A-EMD in Fig. 1 shows no change after acid treating and belongs to typical γ-MnO₂ type. But the structure of H-EMD, indicated as pyrolusite-MnO₂, shows great change. The 2θ=22.1° peak shifts from low angle to high angle, and the peaks of 55°–59°

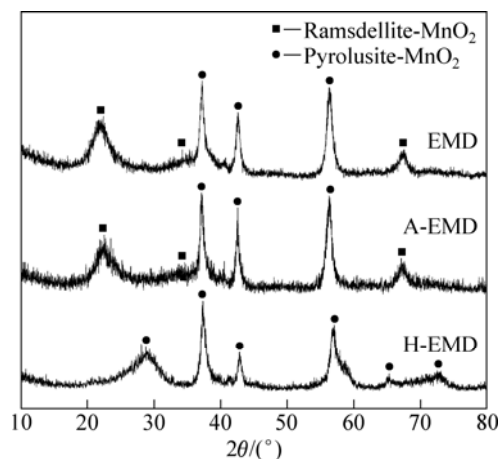


Fig. 1 XRD patterns of EMD, A-EMD and H-EMD

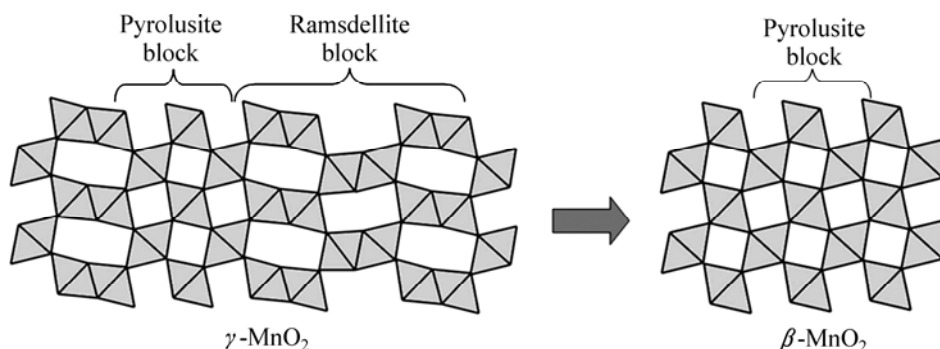


Fig. 2 Structural change scheme of MnO₂

and 64° – 71° split obviously, which indicate that micro-twins defect decreased [14]. After being treated under 400°C for 6 h, the space arrangement of the unit cells is more order and the void area is smaller, γ - MnO_2 (pyrolusite and ramsdellite) is completely transformed into β - MnO_2 (pyrolusite, shown in Fig. 2). Compared with EMD (γ - MnO_2), it may be easier for H-EMD (β - MnO_2) to transform into LiMn_2O_4 . PISTOIA et al [15] believed that the force to propel Li- MnO_2 transforming into spinel LiMn_2O_4 is the electrostatic interaction between Li ions and its adjacent octahedral Mn ions. Pyrolusite (β - MnO_2) possesses a narrower void tunnel structure and shorter spacing distance between Li^+ and Mn^{4+x} , which is beneficial for the shift of Mn ions to void spaces and for the transformation into spinel structure.

The structure of C-EMD is complex, which can be observed from Fig. 3. After being impregnated with chromic salt and pretreated under high temperature, the impregnated Cr^{2+} in EMD is oxidized to Cr_2O_3 , whose diffraction peaks can be observed in Fig. 3. At the same time, Mn^{4+} is partly reduced to lower valence state. Not only β - MnO_2 but also a new phase Mn_3O_4 appears in the XRD patterns of C-EMD.

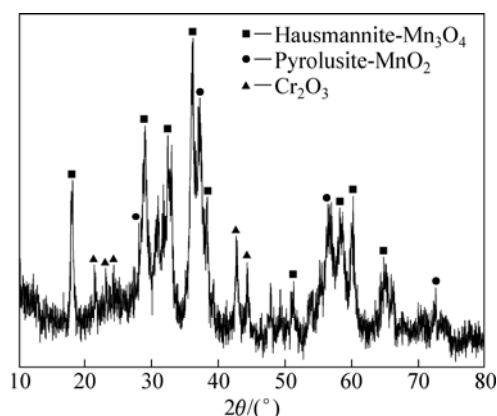


Fig. 3 XRD pattern of C-EMD

Table 1 shows the content analysis of major elements of EMD pretreated by different methods. Compared with the untreated EMD, the Na content in A-EMD decreases from 0.290% to 0.068%, with the reduced degree up to 76.66%. It owes to the exchange of Na^+ and H^+ and a mass of Na^+ escaping from the pores of MnO_2 during the acid treatment. Meanwhile, S content also decreases by 23.13%. And the decrease of impurities raises the Mn content from 59.243% to 60.545%. To H-EMD, the impurities contents, such as Na and S, remain almost unchanged, but the Mn content increases obviously. This is mainly due to the elimination of water and other organic impurities under high temperature. To C-EMD, the Mn content raises because MnO_2 is partly reduced to Mn_3O_4 .

Table 1 Elemental analyses of EMD pretreated by different methods

Sample	w(Mn)/%	w(Cr)/%	w(Na)/%	w(S)/%
EMD	59.243	—	0.290	0.402
A-EMD	60.545	—	0.068	0.309
H-EMD	61.737	—	0.295	0.397
C-EMD	62.655	3.416	0.306	0.311

3.2 Effect of EMD pretreatment on structure and performance of LiMn_2O_4

The XRD patterns of LiMn_2O_4 samples prepared by the above different kinds of EMD are shown in Fig. 4. The diffraction peaks of all the samples belong to pure cubic spinel LiMn_2O_4 type, in which Li and Mn occupy the tetrahedral 8a and octahedral 16d sites, respectively. The calculated lattice parameters for EMD-LMO, A-EMD-LMO, H-EMD-LMO and C-EMD-LMO are 0.8226, 0.8231, 0.8226 and 0.8221 nm respectively.

The lattice parameters of EMD-LMO and H-EMD-LMO are very close. A-EMD-LMO shows the largest lattice parameters, which may be due to the decrease of impure Na content. HE [16] found that Na^+ could substitute the tetrahedral Li^+ in spinel structure and part of Li^+ ions shift to the octahedral Mn^{3+} , which forms $[\text{Na}_\delta\text{Li}_{1-\delta}]_{8a}[\text{Li}_\delta\text{Mn}_{2-\delta}]_{16d}\text{O}_4$. The impure Na^+ decreases the Mn^{3+} content. So, the lattice shrinks and the parameters decrease. Reversely, the decrease of Na^+ content in A-EMD-LMO increases the lattice parameters. No impurity phase of Cr is found in the pattern of C-EMD-LMO, which shows that solid solution $\text{LiCr}_{0.05}\text{Mn}_{1.95}\text{O}_4$ is formed in the sample. Meanwhile, Cr^{3+} with a smaller ionic radius substitutes Mn^{3+} partly, which decreases the lattice parameters, and improves the stability of the structure [17].

Figure 5 shows the initial charge–discharge curves of LiMn_2O_4 obtained from EMD pretreated by different methods. As a reference, EMD-LMO has an initial discharge capacity of 118.7 mA·h/g. A-EMD-LMO has the highest discharge capacity of 125.5 mA·h/g because

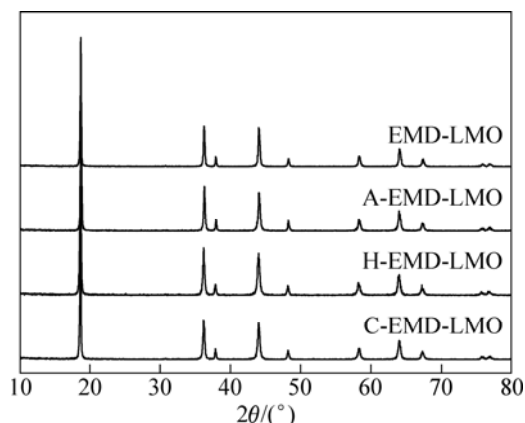


Fig. 4 XRD patterns of as-prepared samples

the Na^+ content decreases after acid treating, which hence decreases cation mixing degree in spinel LiMn_2O_4 and increases the Li^+ amount for deintercalation [18]. H-EMD-LMO has a capacity of 122.6 mA·h/g, which is a little higher than that of the untreated sample. And the capacity of C-EMD-LMO decreases to 110.9 mA·h/g mainly because Cr substitutes Mn sites partly, thus decreasing the Mn^{3+} amount and capacity of the spinel.

Figure 6 shows the cycleability curves of LiMn_2O_4 obtained from EMD pretreated by different methods. As for the LiMn_2O_4 samples from the untreated EMD, A-EMD, H-EMD and C-EMD, the capacity retention ratios after 40 cycles under room temperature keeps 82%, 74.9%, 84.5% and 93.1% respectively. A-EMD-LMO has the highest discharge capacity but the worse cycleability, which may be due to the decrease of Na content in EMD. MITSUI and PANASONIC believed that the residual Na in the EMD is beneficial to the cycleability of as-prepared LiMn_2O_4 [19]. C-EMD-LMO has the best cycleability mainly because the impregnated Cr^{3+} shrinks the lattice and improves the stability of the structure [20,21]. Meanwhile, the decrease of Mn^{3+} is beneficial to the suppression of Jahn-Teller distortion and improvement of the cycleability of as-prepared LiMn_2O_4 .

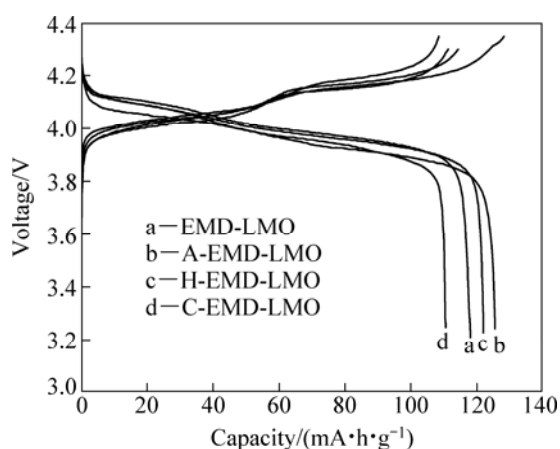


Fig. 5 Initial charge-discharge curves of as-prepared samples

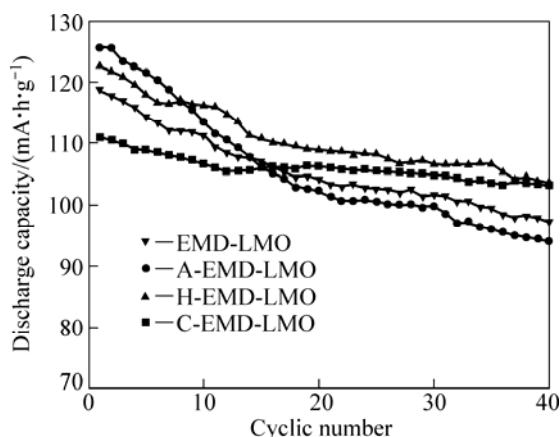


Fig. 6 Cycling performance of as-prepared samples

4 Conclusions

1) Pretreatment of EMD has a certain effect on the as-prepared LiMn_2O_4 : acid treating can decrease the contents of impurities and increase the initial discharge capacity, but the cycleability is deteriorated.

2) After presintering, the water and content of organic impurities infused into EMD decrease and its crystal structure transforms from γ -type to β -type, which decreases the crystal defect and is beneficial to the formation of spinel structure, and therefore, the structural stability and electrochemistry performance of the as-prepared LiMn_2O_4 are improved.

3) To C-EMD, the initial discharge capacity decreases, but the stability and cycleability of the as-prepared LiMn_2O_4 improve greatly.

References

- [1] TANG S B, LAI M O, LU L. Li-ion diffusion in highly (003) oriented LiCoO_2 thin film cathode prepared by pulsed laser deposition [J]. *Journal of Alloys and Compounds*, 2008, 449(1–2): 300–303.
- [2] NIMISHA C S, GANAPATHI M, MUNICHANDRAIAH N, RAO G M. Study on target conditioning for depositing LiCoO_2 thin films [J]. *Vacuum*, 2009, 83(6): 1001–1006.
- [3] KIM C J, AHN I S, CHO K K, LEE S G, CHUNG J K. Characteristics of LiNiO_2 thin films synthesized by Li diffusion on the surface oxidized epitaxial layer of Ni-alloy [J]. *Journal of Alloys and Compounds*, 2008, 449(1–2): 335–338.
- [4] FERGUS J W. Recent developments in cathode materials for lithium ion batteries [J]. *Journal of Power Sources*, 2010, 195(4): 939–954.
- [5] GOODENOUGH J B. Cathode materials: A personal perspective [J]. *Journal of Power Sources*, 2007, 174(2): 996–1000.
- [6] CHEN Ze-hua, HUANG Ke-long, LIU Su-qin, WANG Hai-yan. Preparation and characterization of spinel of LiMn_2O_4 nanorods as lithium-ion battery cathodes [J]. *Transactions of Nonferrous Metals Society of China*, 2010, 20(12): 2309–2313.
- [7] MICHALSKA M, LIPINSKA L, MIRKOWSKA M, AKSIENIONEK M, DIDUSZKO R, WASUCIONEK M. Nanocrystalline lithium-manganese oxide spinels for Li-ion batteries — Sol-gel synthesis and characterization of their structure and selected physical properties [J]. *Solid State Ionics*, 2011, 188(1): 160–164.
- [8] XIONG L, XU Y, TAO T, GOODENOUGH J B. Synthesis and electrochemical characterization of multi-cations doped spinel LiMn_2O_4 used for lithium ion batteries [J]. *Journal of Power Sources*, 2012, 199(1): 214–219.
- [9] ZHOU W J, BAO S J, HE B L, LIANG Y Y, LI H L. Synthesis and electrochemical properties of $\text{LiAl}_{0.05}\text{Mn}_{1.95}\text{O}_4$ by the ultrasonic assisted rheological phase method [J]. *Electrochimica Acta*, 2006, 51(22): 4701–4708.
- [10] XIAO L F, ZHAO Y Q, YANG Y Y, CAO Y L, AI X P, YANG H X. Enhanced electrochemical stability of Al-doped LiMn_2O_4 synthesized by a polymer-pyrolysis method [J]. *Electrochimica Acta*, 2008, 54(2): 545–550.
- [11] LI Xiang-qun, WANG Zhi-xing, LIANG Ru-fu, GUO Hua-jun, LI Xin-hai, CHEN Qi-yuan. Electrochemical properties of high-power lithium ion batteries made from modified spinel LiMn_2O_4 [J].

- Transactions of Nonferrous Metals Society of China, 2009, 19(6): 1494–1498.
- [12] JIANG Qing-lai, HU Guo-rong, PENG Zhong-dong, DU Ke, LIU Ye-xiang. Influence of MnO_2 materials on performance of spinel LiMn_2O_4 prepared by solid state method [J]. Journal of Functional Materials, 2010, 41(9): 1485–1489. (in Chinese)
- [13] XIA Xi. Crystal structure, preparation and discharge performance for manganese dioxides and related manganese oxides (I) [J]. Battery Bimonthly, 2004, 34(6): 411–414. (in Chinese)
- [14] CHABRE Y, PANNETIER J. Structural and electrochemical properties of the proton γ - MnO_2 system [J]. Progress in Solid State Chemistry, 1995, 23(1): 1–130.
- [15] PISTOIA G, ANTONINI A, ZANE D, PASQUALI M. Synthesis of Mn spinels from different polymorphs of MnO_2 [J]. Journal of Power Sources, 1995, 56(1): 37–43.
- [16] HE Fang-yong. Study on synthesis and properties of doped lithium manganese oxide [D]. Changsha: Central South University, 2007. (in Chinese)
- [17] PENG Z D, JIANG Q L, DU K, WANG W G, HU G R, LIU Y X. Effect of Cr-sources on performance of $\text{Li}_{1.05}\text{Cr}_{0.04}\text{Mn}_{1.96}\text{O}_4$ cathode materials prepared by slurry spray drying method [J]. Journal of Alloys and Compounds, 2010, 493(1–2): 640–644.
- [18] GUO Hua-jun, LI Xiang-qun, HE Fang-yong, LI Xin-hai, WANG Zhi-xing, PENG Wen-jie. Effects of sodium substitution on properties of LiMn_2O_4 cathode for lithium ion batteries [J]. Transactions of Nonferrous Metals Society of China, 2010, 20(6): 1043–1048.
- [19] NAGAYAMA M, ARIMOTO S, NUMATA K. Production method of spinel lithium manganese oxides, the cathode materials and nonaqueous secondary battery: CN Patent, 99801152.5 [P]. 1999–06–08. (in Chinese)
- [20] YU Ze-min, ZHAO Lian-cheng. Preparation and electrochemical properties of $\text{LiMn}_{1.95}\text{M}_{0.05}\text{O}_4$ ($\text{M}=\text{Cr}, \text{Ni}$) [J]. Rare Metals, 2007, 26(1): 62–67.
- [21] JIANG Qing-lai, HU Guo-rong, PENG Zhong-dong, DU Ke, CAO Yan-bing, TANG Dai-chun. Preparation of spherical spinel $\text{LiCr}_{0.04}\text{Mn}_{1.96}\text{O}_4$ cathode materials based on slurry spray drying method [J]. Rare Metals, 2009, 28(6): 618–623.

电解二氧化锰预处理对制备锰酸锂性能的影响

赵于前¹, 蒋庆来², 王伟刚³, 杜柯³, 胡国荣³

1. 中南大学 地球科学与信息物理学院, 长沙 410083;
2. 中南大学 粉末冶金研究院, 长沙 410083;
3. 中南大学 冶金科学与工程学院, 长沙 410083

摘 要: 分别采用酸洗、预烧、浸渍掺铬的方式对电解二氧化锰(EMD)进行预处理, 研究 EMD 预处理对制备锰酸锂性能的影响。采用 XRD、ICP 等手段对预处理的 EMD 及制备的锰酸锂进行表征, 并通过 $\text{Li}/\text{LiMn}_2\text{O}_4$ 电池的充放电测试对其电化学性能进行评估。结果表明, 酸洗后 EMD 中的钠、硫等无机杂质含量显著降低; 预烧能够有效去除 EMD 吸附的水分和有机杂质, 扩大孔径, 增多反应活性位点; 对 EMD 进行浸渍掺铬的预处理, 能够得到更加均质的掺铬锰酸锂材料 $\text{LiCr}_{0.05}\text{Mn}_{1.95}\text{O}_4$, 并表现出较好的结构稳定性及容量保持率。

关键词: 锂离子电池; 正极材料; 锰酸锂; 二氧化锰

(Edited by YANG Hua)